

AlPO₄-coated mullite/alumina fiber reinforced reaction-bonded mullite composites

Yahua Bao*, Patrick S. Nicholson

Ceramic Engineering Research Group, Department of Materials Science and Engineering, McMaster University, Hamilton, Ontario, L8S 4L7 Canada

Received 23 February 2008; received in revised form 27 May 2008; accepted 30 May 2008

Available online 22 July 2008

Abstract

A precursor for reaction-bonded mullite (RBM) is formulated by premixing Al₂O₃, Si, mullite seeds and mixed-rare-earth-oxides (MREO). An ethanol suspension thereof is stabilized with polyethyleneimine protonated by acetic acid. The solid in the suspension is infiltrated into unidirectional mullite/alumina fiber-preforms by electrophoretic infiltration deposition to produce fiber-reinforced, RBM green bodies. Crack-free composites with ≤25% porosity were achieved after pressureless sintering at 1300 °C. Pre-coating the fibers with AlPO₄ as a weak intervening layer facilitates significant fiber pullout on composite fracture and confers superior damage tolerance. The bend strength is ~170 MPa at 25 °C ≤ T ≤ 1100 °C. At 1200 °C, the composite fails in shear due to MREO-based, glassy phase formation. However, the AlPO₄ coating acts as a weak layer even after thermal aging at 1300 °C for 100 h.

© 2008 Elsevier Ltd. All rights reserved.

Keywords: AlPO₄; Weak layer; Nextel 720 fiber; Reaction-bonded mullite; Ceramic matrix composites

1. Introduction

Fiber-reinforced ceramic matrix composites (CMC's) are candidates for structural application due to their damage tolerance. Currently, most dense fiber-reinforced CMC's are based on non-oxide systems which oxidize in air at high temperatures. Oxidation-resistant, fiber-reinforced CMC's are required for use in oxidizing atmospheres at high temperatures. To optimize the fracture work necessary to break fiber-reinforced CMC's, the bonding between fiber and matrix must allow fiber pullout from the matrix via a weak layer therebetween.¹ LaPO₄ has been reported as one of the most successful dense weak layer candidates.^{2–4} However, Bao and Nicholson⁵ recently reported application of another phosphate, AlPO₄, as the weak layer on the fiber surface. They demonstrated significant fiber pullout on the fracture surface of hot-pressed, AlPO₄-coated mullite/alumina (Nextel™ 720) fiber-reinforced Al₂O₃. Highly covalently-bonded AlPO₄ displays poor sintering behavior even sintered at 1550 °C.⁵ Thus it should be a stable porous weak

layer on fiber surface for crack deflection and fiber pullout. Use of a reaction-bonded matrix with near-zero sintering shrinkage should avoid the necessity to hot-press.

Mullite is an ideal matrix at elevated temperatures because of high temperature strength, low thermal expansion coefficient and good creep resistance. Due to the volume stability of mullite/alumina fibers, the matrix sintering shrinkage must be low to avoid cracks on pressureless sintering. Reaction-bonded mullite (RBM) explored as near-zero shrinkage is achieved by mixing alumina, silicon and aluminum precursors.^{6–8} In reaction-bonded mullite of composition 3Al₂O₃–2Si, the precursor Si oxidizes to SiO₂ at high temperatures which reacts with the Al₂O₃ to form mullite. Two volume expansion reactions are involved, i.e., Si → SiO₂ (+134%), and 3Al₂O₃–2SiO₂ → mullite (+1.3%). The reaction shrinkage can be theoretically calculated as;

$$s = 1 - \left(1.013 + \frac{1.340 \times 1.013 \times V_{\text{Si}} \rho_0}{V_{\text{Al}_2\text{O}_3} + V_{\text{Si}} \rho} \right)^{1/3} \quad (1)$$

where ρ_0 and ρ are the theoretical-green and fired-densities ($V_{\text{Al}_2\text{O}_3}$ and V_{Si} are the volume fractions of Al₂O₃ and Si powder in the mixture, respectively). Generally, after green processing, the ceramic density is ~55%. For 3% sintering shrinkage,

* Corresponding author. Current address: SII MegaDiamond, 275 West 2230 North, Provo, UT 84604, United States.

E-mail address: baoyahua@gmail.com (Y. Bao).

the fired density can be 80% theoretical. Thus reaction-bonded-mullite with less than 20% porosity and less than 3% shrinkage should not be problem if the SiO₂ comes from the Si precursor, i.e., fiber-reinforced, reaction-bonded-mullite composites can be realistically fabricated by pressureless sintering free of macro cracks. The mullite-formation temperature is ~1500 °C, however, the strength of the mullite/alumina (Nextel™ 720) fiber degrades severely on heat-treatment >1300 °C.⁹ Thus the mullite matrix sintering temperature must be modified to ≤1300 °C for fiber strength retention. Recently, rare earth oxides added to RBM reduced the mullite-formation temperature to 1350 °C.¹⁰ So mixed-rare-earth-oxides (MREO) were added to the RBM mixture to form mullite <1300 °C.¹¹

In this paper, AlPO₄-coated, Nextel 720 fiber/reaction-bonded mullite composites are fabricated by constant-current electrophoretic-infiltration-deposition (EPID) and subsequently pressureless-sintered.

2. Experimental

Reaction-bonded mullite was prepared with submicron TM-DAR alumina powder (Taimei Chemicals, Tokyo, Japan) and micron Si metal powder (Atlantic Equipment Engineers, Nergenfield, NJ) which was pre-ball-milled in ethanol to a surface area >20 m²/g (to promote oxidation during sintering). Table 1 lists composition of mixed-rare-earth-oxides (MREO, Lanthanide oxide, Molycorp, Fairfield, NJ). These were added as sintering and mullite-formation aids. A mullite precursor (Siral 28 M, SASOL GmbH, Hamburg, German), pre-sintered at 1300 °C for 2 h to form pure mullite, was ground and added as mullite-promotion seeds. The molar ratio of Al:Si was set to that of mullite.

Anhydrous polyethyleneimine dispersant (PEI, M.W. 10,000, Polysciences, Warrington, PA), protonated with glacial acetic acid was added to stabilize the RBM-precursor, ethanol suspension. The optimal addition was determined via the electrophoretic mobility value for the RBM precursors with a zeta potential analyzer (ZetaPALS, Brookhaven Instruments, Holtsville NY). The electrokinetic sonic amplitude (ESA) was measured on the mixed suspension (ESA-8000, Matec Applied Sciences, Hopkinton, MA). RBM pellets were also uniaxially pressed then cold isostatically pressed at 140 MPa and heated to 1175–1200 °C for 10 h in air to oxidize the Si to SiO₂. Finally they were sintered at 1250–1350 °C for 2 h to study mullite phase formation and shrinkage. Shrinkage was calculated from the change of the diameter of the pellets.

Table 1
Composition of the mixed-rare-earth-oxides (MREO) provided by Molycorp

Oxide	Concentration (wt%)
CeO ₂	49
La ₂ O ₃	33
Nd ₂ O ₃	13
Pr ₆ O ₁₁	4
Other	1

AlPO₄ was coated onto the mullite/alumina fibers (Nextel™ 720, 3 M, St. Paul, MN) by a layer-by-layer electrostatic method.⁵ Desized fibers were pre-treated with 0.5 wt% cationic polyelectrolyte solution (polydiallyldimethylammonium chloride, Aldrich, M.W. 400,000–500,000) to induce a positive surface charge. The latter attracts the negatively-charged AlPO₄ nano-particles to produce the coating. The coated fibers were heat-treated at 1100 °C. AlPO₄ was coated for 10 cycles (~10 wt% gain) to give an acceptable thickness. The coated fibers were unidirectionally mounted in a rectangular, plastic holder (25 mm × 5 mm × 3 mm), the back of which was attached to a metal plate as cathode to draw particles through the fiber preform and accomplish electrophoretic-infiltration-deposition (EPID).^{12,13} The inter-electrode distance was 2 cm and EPID was conducted at a constant current of 0.07 mA/cm². After deposition, the composite was cold isostatically pressed at 140 MPa then dried in an atmosphere-controlled closed container to avoid cracking. Uncoated fibers were also infiltrated with RBM matrix for comparison.

The green composites were heated to 1175 °C for 10 h in air to convert the Si to SiO₂ then sintered at 1300 °C for 2 h. Their thermal stability was determined by heat-treatment for 100 h at 1300 °C. The fired density and open porosity were measured by Archimedes' method in water.

Four-point bend testing was performed at 0.10 mm/min in a screw-driven, ultra-hard compression machine (Model 10053 & 10055, Wykeham Farrance Engineering Ltd., UK) using an alumina fixture with outer span, 20 mm, and inner span, 10 mm. The sample thickness was 2.0–2.5 mm. Fracture surfaces were observed by SEM and the degree of fiber-pullout determined. Ten samples were tested at room temperature and five at elevated temperatures.

3. Results and discussion

Fig. 1 shows the DTA curve for 32 wt% MREO, 22 wt% Al₂O₃ and 46 wt% SiO₂ mixture. The endothermic peak around 1200 °C is due to eutectic liquid-phase formation. Mullite phase can be promoted by formation of the MREO–Al₂O₃–SiO₂ eutectic liquid phase. Fig. 2 tracks the phase evolution in the RBM matrix versus sintering temperature for a mixture containing 7.5 wt% MREO. Mullite appears at 1270 °C, and is the major phase at 1300 °C. Traces of alumina and silica remain. The sil-

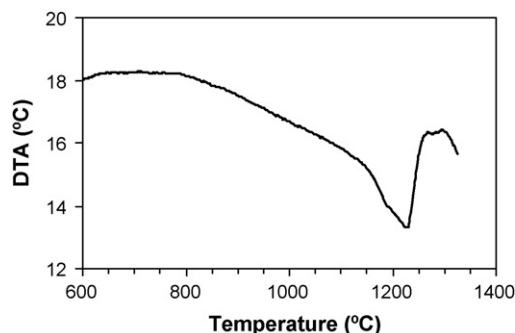


Fig. 1. DTA curve for 32 wt% MREO, 22 wt% Al₂O₃ and 46 wt% SiO₂ mixture.

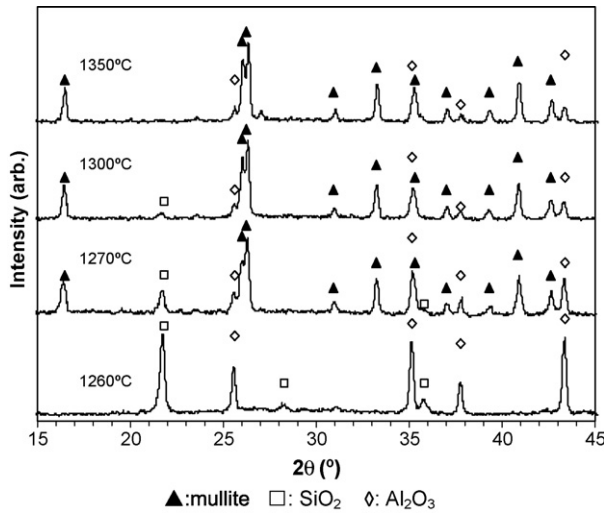


Fig. 2. Phase evolution of the reaction-bonded mullite containing 7.5 wt% MREO.

ica is totally consumed >1300 °C but the alumina trace persists. The mullitization temperature was further decreased by adding mullite “seeds” (Fig. 3). With 0.5 wt% seeds, the mullitization process was complete at 1270 °C. However, the sintering shrinkage (6–8%) was still too large (should be <~3% to avoid matrix cracks around the volume stable fibers). Fig. 4 tracks the effect of mullite seed content on the shrinkage, density and open porosity, for RBM with 7.5 wt% MREO. A small amount of mullite seeds can prompt the formation of mullite. However, when seed concentration is high, it serves as refractory inclusion and retards the RBM sintering. Fig. 5 shows the dilatometric measurement curve for RBM with 7.5 wt% MREO and 5.0 wt% seeds. Length expansion occurs due to oxidation of Si metal powder and reaches maximum (<3%) at 1170 °C, close to the eutectic point of MREO–Al₂O₃–SiO₂. Formation of MREO–Al₂O₃–SiO₂ liquid phase prompts the sintering shrinkage and a steep drop in length was detected at 1170–1200 °C. Si metal is completely oxidized into silica when soaked at 1200 °C for 10 h. With further

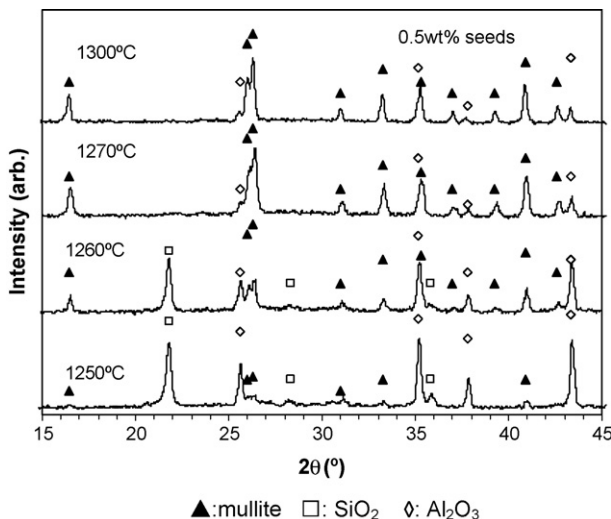


Fig. 3. Effect of mullite seed addition on the mullitization temperature.

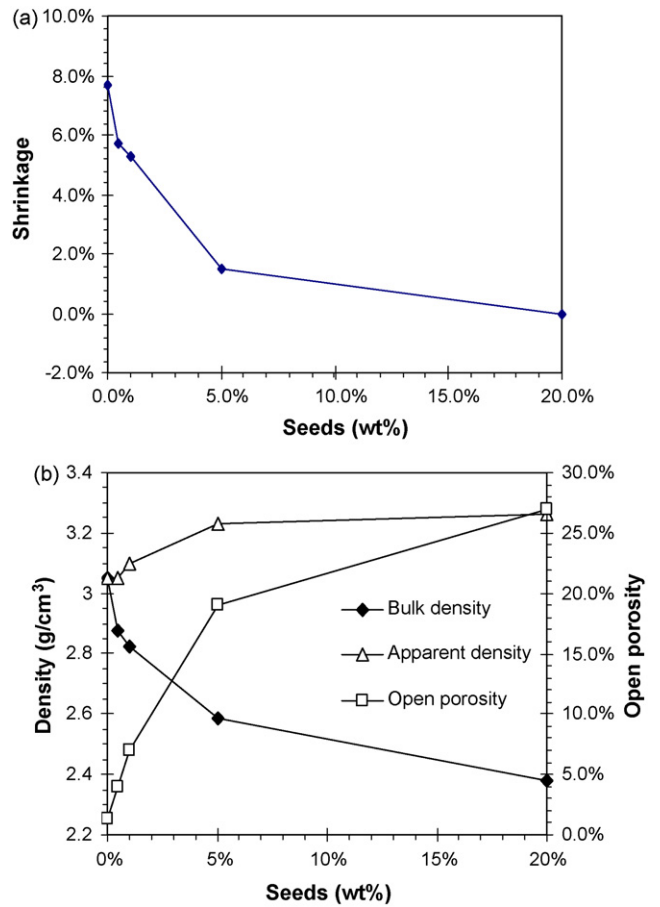


Fig. 4. Influence of mullite seed addition on the sintering shrinkage, density and open porosity for RBM sintered at 1300 °C for 2 h.

increase of temperature, RBM sintering shrinkage takes place and final length change is <3%. When [seeds] = 5 wt%, the RBM shrinkage is <3% and open porosity, <20%. This composition is optimum and is used in the EPID processing.

Alumina particles in ethanol are positively charged whereas Si particles are negatively charged. These particles tend to hetero-coagulate. A dispersant was added to induce a common surface charge sign and stabilize the mixed suspension. PEI, protonated with acetic acid, adsorbs on both surfaces ren-

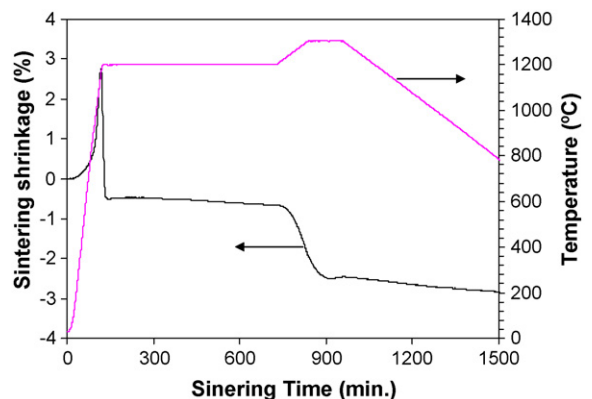


Fig. 5. Dilatometric measurement of RBM with 7.5 wt% MREO and 5.0 wt% seeds.

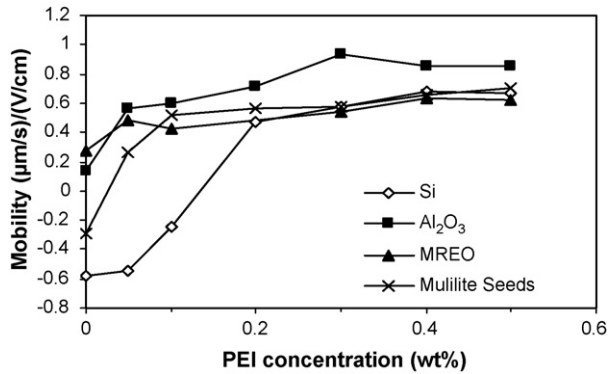


Fig. 6. Effect of PEI on mobility.

dering them the same sign. Fig. 6 illustrates the influence of PEI on the RBM-precursor-particle-mobility in ethanol. When $[\text{PEI}] > 0.15$ wt%, all particles are positively charged. No change of particle mobility is observed for $[\text{PEI}] > 0.4$ wt%. Fig. 7 shows the electrokinetic sonic amplitude (ESA) values for a 2.5 vol% mixed suspension of alumina, Si, MREO and mullite seeds ($3\text{Al}_2\text{O}_3-2\text{Si}+5$ wt% mullite seeds + 7.5 wt% MREO) versus PEI concentration. The ESA value increases with PEI and plateaus at $[\text{PEI}] > 0.3$ wt%. Thus 0.5 wt% PEI was used to ensure well-dispersed suspensions for the EPID process. As PEI also adsorbs on the AlPO_4 -coated fiber surface, it renders the fibers repulsive to the particles. The fiber adsorption of PEI causes particles passing through them to be repelled as they pass, i.e., particles are “streamed”.

Fig. 8 shows the morphology of an AlPO_4 -coated Nextel 720 fiber-reinforced composite prepared by EPID (current density 0.07 mA/cm^2) pressurelessly sintered at 1300°C for 2 h. Sintered fiber-reinforced composites have $\sim 25\%$ open porosity and ~ 25 vol% fiber. Macro cracks do not occur and particles are well infiltrated into the fiber preform. After polishing, the weakly-bonded AlPO_4 coating polished away and grooves appeared around the fibers. An uncoated Nextel 720/RBM composite was employed for matrix phase analysis due to the very similar XRD patterns for AlPO_4 and SiO_2 . Fig. 9 is an XRD pattern for uncoated Nextel 720 Fiber/RBM composite sintered at 1300°C

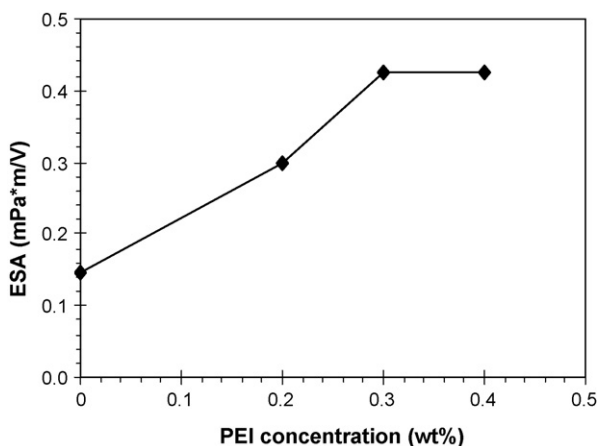


Fig. 7. Effect of PEI on ESA of 2.5 vol% suspension.

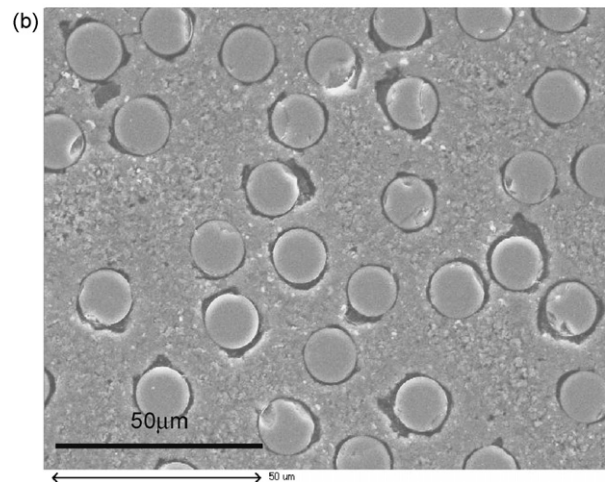
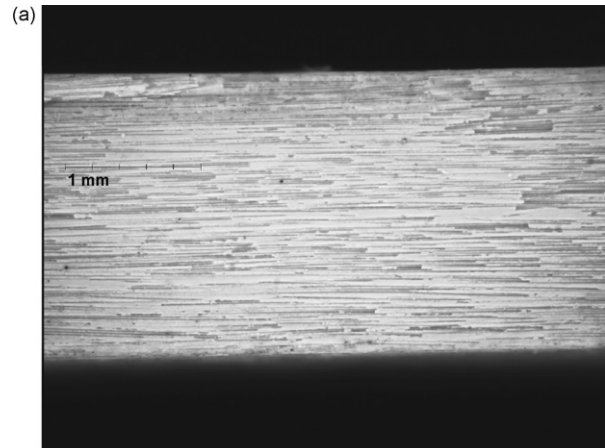
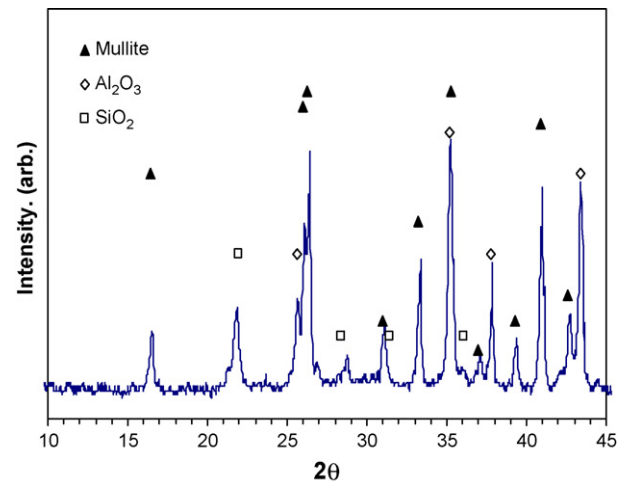


Fig. 8. Morphology of fiber/RBM composite prepared by EPID.

for 2 h. It is a mixture of alumina, cristobalite and mullite, suggesting non-uniform distribution of the MREO in the matrix. MREO promotes matrix mullite formation via low temperature eutectics formed with alumina and silica.¹¹ As the MREO powder has high density, it also may sediment during fiber preform

Fig. 9. X-ray diffraction pattern of fiber/RBM composite prepared by EPID and sintered at 1300°C .

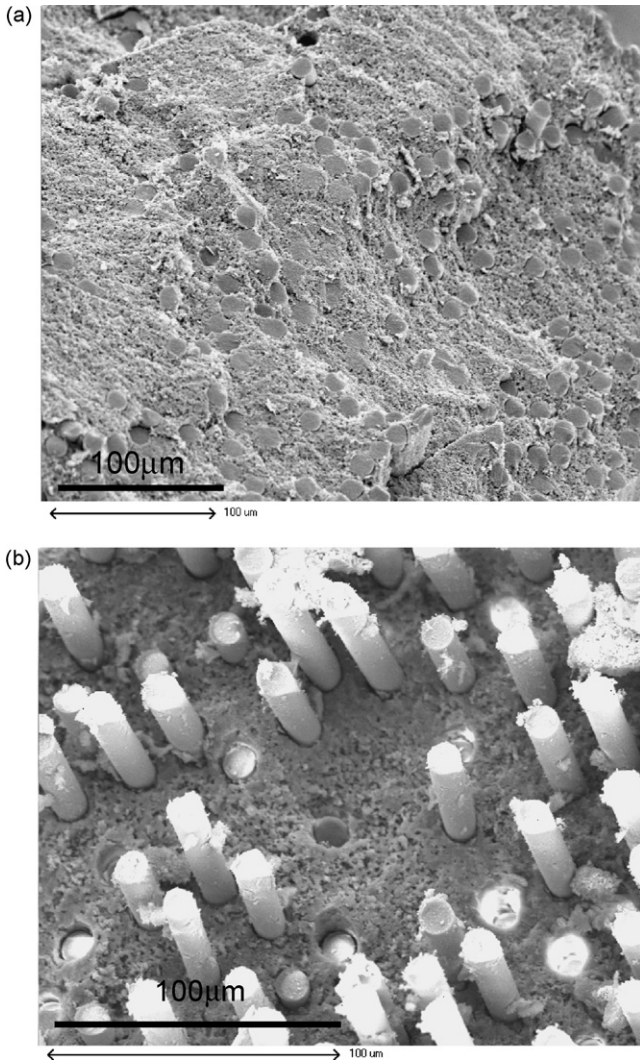


Fig. 10. Effect of AlPO₄ coating on fracture surface of fiber/RBM composites tested at R.T. (a) without AlPO₄ coating and (b) with AlPO₄ coating.

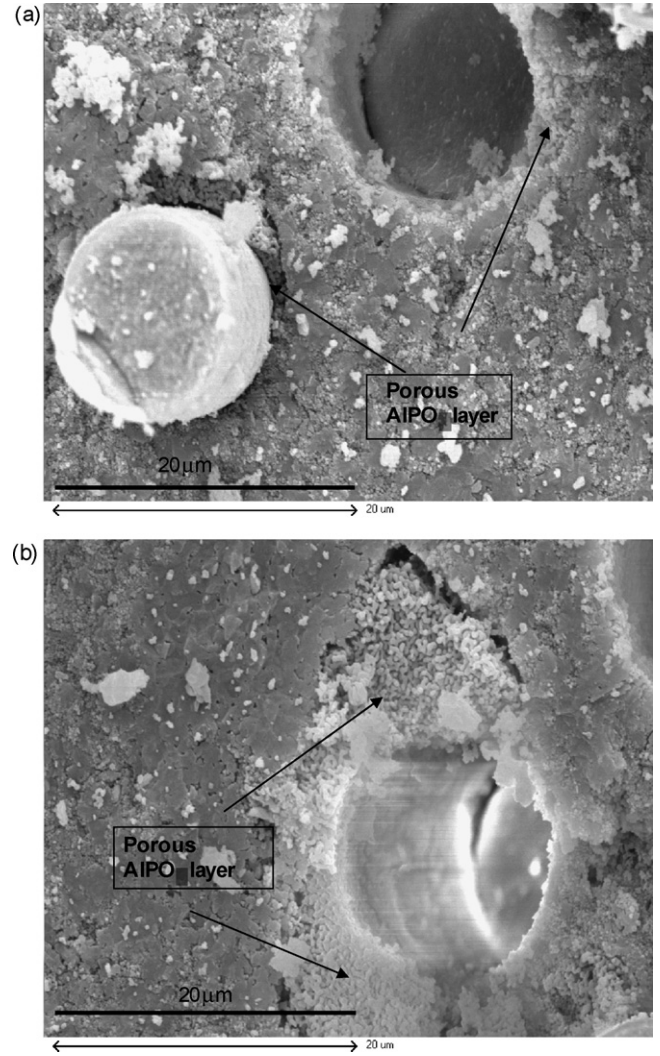


Fig. 11. Porous AlPO₄ coating after sintering at 1300 °C for 2 h.

infiltration. In fact, a yellow layer was noted on the base of a green body after infiltration. A non-uniform distribution, or, less-MREO-present-than-designed will locally retard formation of mullite at 1300 °C.

Fig. 10 compares the effect of AlPO₄-coating on fiber pullout, i.e., without AlPO₄ on the fibers, strong bonds form between the fibers and the RBM matrix so that a planar fracture surface results. However, when AlPO₄ is coated on the fibers, significant fiber pullout is observed. The high covalent bonding level in AlPO₄ retards its sinterability so AlPO₄ ceramics remain very porous even when sintered at 1550 °C.⁵ Thus the inherently-porous AlPO₄ coating on Nextel 720 fiber surface, serves as a porous weak layer for crack deflection and fiber pull-out. Fig. 11 show porous AlPO₄ coating attached to the matrix after the fiber pullout, indicating that the AlPO₄/fiber bonding is also weak and cracks deflect therefrom. Fig. 12 illustrates the fiber bridging effect. Though the crack opening distance is ~150 μm, the fibers still bridge across it. Fiber pullout reaches ~150 μm (>10 times the fiber diameter). The pullout length is shorter on fracture at 1100 °C (Fig. 13). Fig. 14 shows the

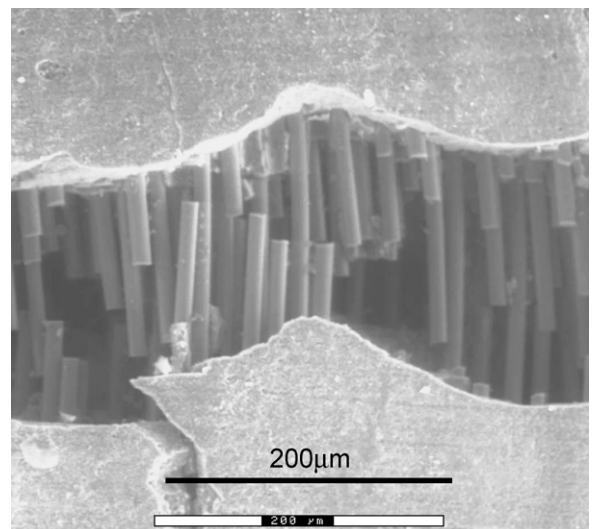


Fig. 12. Fiber bridging and pullout across a matrix crack in AlPO₄-coated fiber/RBM composite tested at room temperature.

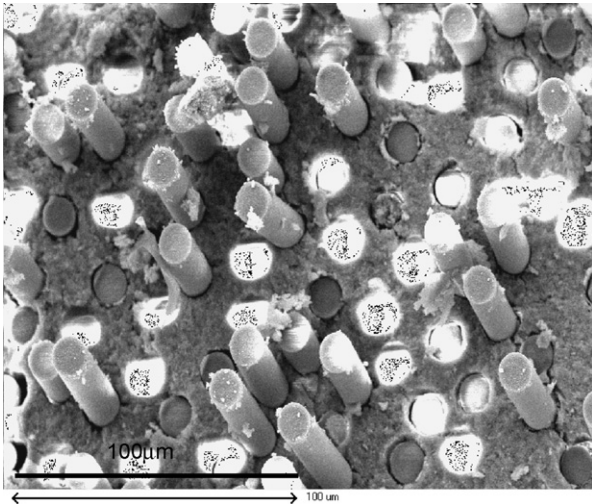


Fig. 13. Fracture surface of AlPO₄-coated-fiber/RBM composite with AlPO₄ weak layer tested at 1100 °C.

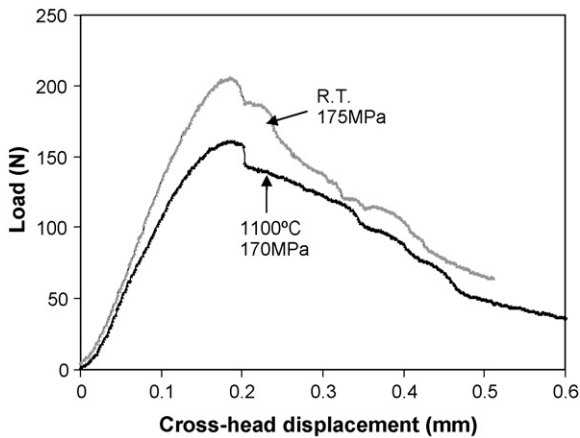


Fig. 14. 4-point bending strength of AlPO₄-coated-fiber/RBM composites tested at R.T. and 1100 °C.

load/cross-head-displacement curves for the composite tested at room temperature and 1100 °C. The composite exhibits damage tolerance at both temperatures. The ultimate bend strength of the composite is 175 ± 20 MPa and 170 ± 25 MPa at room temperature and 1100 °C, respectively. At 1200 °C, the MREO-induced MREO–Al₂O₃–SiO₂ glassy phase occurs in the matrix, thus the composite fails in shear at 1200 °C (Fig. 15). The ultimate bend strength of RBM and AlPO₄-coated fiber/RBM is listed in Table 2.

Antti et al.¹⁴ reported thermal degradation of commercial fiber reinforced porous aluminosilicate matrix composites. After

Table 2
The bend strengths of RBM and AlPO₄-coated Nextel 720 fiber/RBM composites

Sample	Bend strength (MPa)		
	25 °C	1100 °C	1200 °C
RBM	105 ± 15	70 ± 10	17 ± 5
AlPO ₄ -coated fiber/RBM	175 ± 20	170 ± 25	Shear failure

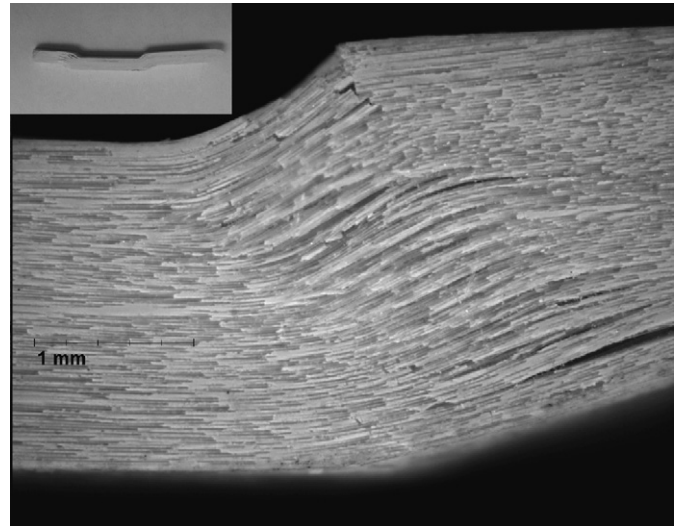


Fig. 15. A morphology of an AlPO₄-coated-fiber/RBM composite tested at 1200 °C.

exposure at 1100 °C in air, the composite embrittles due to localized matrix densification and increased bonding of fibers therewith. Although the RBM matrix is still with $\sim 20\%$ porosity, the composite thermal stability can be significantly increased with AlPO₄ weak layer coating. Fig. 16 shows the load/cross-head-displacement curve for an AlPO₄-coated Nextel 720/RBM composite after heat-treatment at 1300 °C for 100 h. The composite still exhibits damage tolerance with a bend strength of 160 MPa. The AlPO₄ coating is still porous (Fig. 17). Almost no AlPO₄ grain growth occurs during heat-treatment at 1300 °C for 100 h. But the fiber pullout length is shorter (Fig. 18). Short fiber pullout length should be mostly due to the severe fiber strength degradation on thermal aging at 1300 °C. The effect of thermal aging on interfacial bonding needs to be further evaluated.

Kriven and Lee¹⁵ proposed phase transformation causes weakening in mullite/cordierite laminates with β -cristobalite (SiO₂) as the interface. The $\alpha \leftrightarrow \beta$, “cristobalite”, AlPO₄

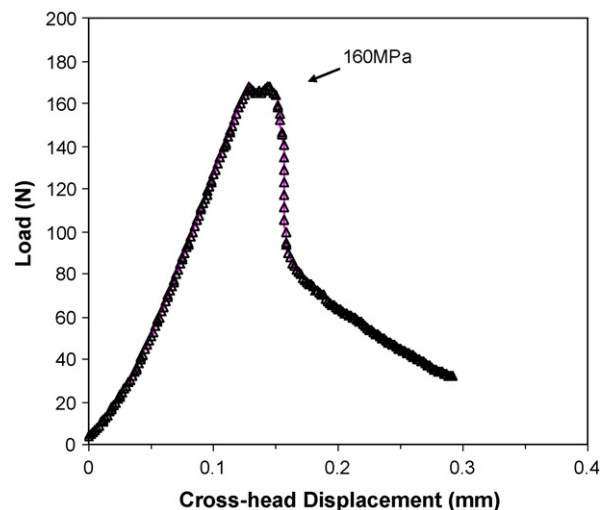


Fig. 16. Load/cross-head displacement curve for AlPO₄-coated-fiber/RBM composite tested at room temperature after heat-treatment at 1300 °C for 100 h.

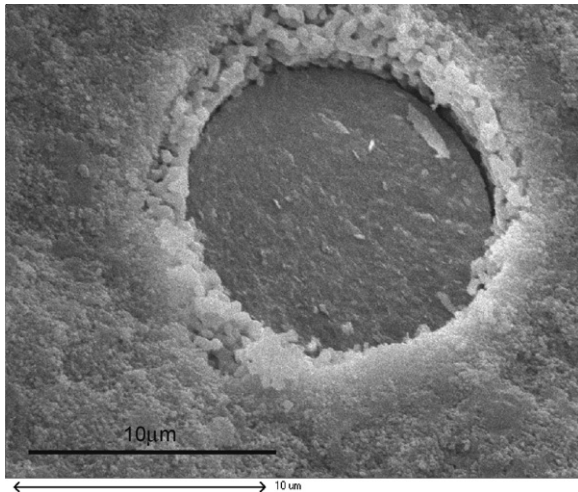


Fig. 17. Porous AlPO_4 coating around fiber after heat-treatment at 1300°C for 100 h.

transformation occurs at 220°C with 4.6% volume change. Microcracks due to the phase transformation are minimized as the coating is porous. The AlPO_4 coating should be pure “ β -cristobalite” phase at 1100°C , however, it will still serve as a weak layer between the fibers and matrix. Thus, phase-transformation weakening in porous AlPO_4 coating can be neglected. The smooth pullout fiber surface and AlPO_4 coating attached to the matrix suggest weak bonding between the fibers and the AlPO_4 coating even after heating to high temperatures. Therefore, an approaching crack will deflect along the fiber/ AlPO_4 surface.

The interfacial sliding resistance depends on the AlPO_4 -coating elastic modulus. A low elastic modulus significantly decreases the fiber/coating sliding resistance, promoting fiber pullout.^{16,17} Elastic modulus is a function of porosity¹⁸;

$$E_p = E(1 - 1.9f_p + 0.9f_p^2)$$

where E and E_p are the elastic modulus of the fully dense and porous materials, respectively and f_p the porosity. The elastic

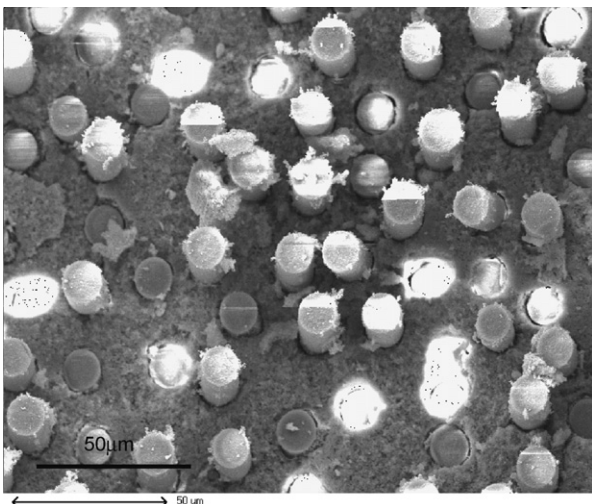


Fig. 18. Fiber pullout after heat-treatment at 1300°C for 100 h, fractured at R.T.

modulus of AlPO_4 is 57 GPa,¹⁹ so, assuming the porosity is approximately that of sintered AlPO_4 , i.e., $\sim 30\%$,⁵ the coating elastic modulus is ~ 29 GPa. This low value explains why significant fiber pullout occurs from the matrix. It can be concluded that the high covalent bonding (poor sinterability) in AlPO_4 is key to its performance on the fiber pullout. The latter results from both the low elastic modulus of porous AlPO_4 coating and the weak bonding between the fibers and the AlPO_4 coating.

4. Summary

Reaction-bonded mullite was formed at $<1300^\circ\text{C}$ via incorporation of 7.5 wt% mixed-rare-earth-oxides into an Al_2O_3 -Si mixture. Inclusion of 5 wt% mullite seeds decreased the sintering shrinkage to $<2\%$ and give a density ~ 2.6 g/cm³ with open porosity $<20\%$. A PEI dispersant produced a stable ethanol suspension of the reaction-bonded mullite precursor. Crack free, unidirectional fiber-reinforced RBM composites with 25 vol% fibers and 25% porosity were achieved by EPID followed by pressureless sintering at 1300°C . AlPO_4 was coated onto mullite/alumina fibers and the fiber/RBM composites exhibited superior damage tolerance with significant fiber pullout between room temperature and 1100°C . The ultimate bend strength of the composites was ~ 170 MPa. At 1200°C , the composite failed in shear due to glassy phase formation in the matrix. The composite still displayed damage tolerance with fiber pullout after thermal aging at 1300°C for 100 h, and testing at room temperature. It is concluded AlPO_4 is an effective oxidation-resistant, weak layer between the fibers and matrix of oxide-fiber/oxide-matrix CMC's.

Acknowledgement

Yahua Bao would like to thank Prof. D.S. Wilkinson and Prof. J. Barbier for fruitful discussions.

References

1. Committee on Advanced Fibers for High-Temperature Ceramic Composites, National Research Council, *Ceramic Fibers and Coatings: Advanced Materials for the Twenty-First Century*. NMAB-494, National Academies Press, Washington, DC, 1998.
2. Morgan, P. E. D. and Marshall, D. B., Ceramic composites of monazite and alumina. *Journal of the American Ceramic Society*, 1995, **78**(6), 1553–1563.
3. Marshall, D. B., Davis, J. B., Morgan, P. E. D., Waldrop, J. R. and Porter, J. R., Properties of La-monazite as an interphase in oxide composites. *Zeitschrift Fur Metallkunde*, 1999, **90**(12), 1048–1052.
4. Kerans, R. J., Hay, R. S., Parthasarathy, T. A. and Cinibulk, M. K., Interface design for oxidation-resistant ceramic composites. *Journal of the American Ceramic Society*, 2002, **85**(11), 2599–2632.
5. Bao, Y. and Nicholson, P. S., AlPO_4 coating on alumina/mullite fibers as a weak interface in fiber-reinforced oxide composites. *Journal of the American Ceramic Society*, 2006, **89**(2), 465–470.
6. Wu, S. X. and Claussen, N., Fabrication and properties of low-shrinkage reaction-bonded mullite. *Journal of the American Ceramic Society*, 1991, **74**(10), 2460–2463.
7. Wu, S. and Claussen, N., Reaction bonding and mechanical properties of mullite/silicon carbide composites. *Journal of the American Ceramic Society*, 1994, **77**(11), 2898–2904.

8. Holz, D., Pagel, S., Bowen, C., Wu, S. and Claussen, N., Fabrication of low-to-zero shrinkage reaction-bonded mullite composites. *Journal of the European Ceramic Society*, 1996, **16**(2), 255–260.
9. Petry, M. D. and Mah, T. I., Effect of thermal exposures on the strengths of NextelTM 550 and 720 filaments. *Journal of the American Ceramic Society*, 1999, **82**(10), 2801–2807.
10. Mechnich, P., Schneider, H., Schmucker, M. and Saruhan, B., Accelerated reaction bonding of mullite. *Journal of the American Ceramic Society*, 1998, **81**(7), 1931–1937.
11. Kim, H. S. and Nicholson, P. S., Use of mixed-rare-earth oxide in the preparation of reaction-bonded mullite at $\leq 1300^\circ\text{C}$. *Journal of the American Ceramic Society*, 2002, **85**(7), 1730–1734.
12. Bao, Y. and Nicholson, P. S., Electrophoretic Infiltration deposition for fiber-reinforced ceramic composites under constant current. *Journal of the American Ceramic Society*, 2007, **90**(4), 1063–1070.
13. Y. Bao, Strong, *Damage-Tolerant Oxide-Fiber/Oxide-Matrix Composites*. Ph.D. Thesis, McMaster University, Hamilton, Ontario, Canada 2006.
14. Antti, M.-L., Lara-Curzio, E. and Warren, R., Thermal degradation of an oxide fibre (Nextel 720)/aluminosilicate composite. *Journal of the European Ceramic Society*, 2004, **24**(3), 565–578.
15. Kriven, W. M. and Lee, S. J., Toughening of mullite/cordierite laminated composites by transformation weakening of beta-cristobalite interphases. *Journal of the American Ceramic Society*, 2005, **88**(6), 1521–1528.
16. Hsueh, C.-H., Becher, P. F. and Angelini, P., Effects of interfacial films on thermal stresses in whisker-reinforced ceramics. *Journal of the American Ceramic Society*, 1988, **71**(11), 929–933.
17. Kerans, R. J., Viability of oxide fiber coatings in ceramic composites for accommodation of misfit stresses. *Journal of the American Ceramic Society*, 1996, **79**(6), 1664–1668.
18. Kingery, W. D., Bowen, H. K. and Uhlmann, D. R., *Introduction to Ceramics*. John Wiley & Sons, New York, 1976.
19. Hanada, T., Bessyo, Y. and Soga, N., Elastic-constants of amorphous thin-films in the systems $\text{SiO}_2\text{-Al}_2\text{O}_3$ and $\text{AlPO}_4\text{-Al}_2\text{O}_3$. *Journal of Non-Crystalline Solids*, 1989, **113**(2–3), 213–220.